Results in Pharma Sciences 2 (2012) 38–45

Contents lists available at SciVerse ScienceDirect

Results in Pharma Sciences

journal homepage: www.elsevier.com/locate/rinphs

Development of oxaliplatin encapsulated in magnetic nanocarriers of pectin as a potential targeted drug delivery for cancer therapy

Raj Kumar Dutta *, Saurabh Sahu

Analytical Chemistry Laboratory, Department of Chemistry, Indian Institute of Technology Roorkee, Roorkee 247667, India

ARTICLE INFO

Article history:
Received 5 May 2012
Accepted 15 May 2012
Available online 22 May 2012

Keywords:
Pectin
SPIONs
Polymer nanocarrier
Oxaliplatin
Controlled release
Targeted drug delivery

ABSTRACT

Superparamagnetic iron oxide nanoparticles (SPIONs) and oxaliplatin (OHP) were in-situ encapsulated in pectin cross-linked with Ca^{2+} forming 100–200 nm sized magnetically functionalized pectin nanocarriers, referred here as MP-OHP nanocarriers. The scanning electron microscopy (SEM) and transmission electron microscopy (TEM) studies revealed formation of spherical nanostructures. The magnetic measurements by vibration sample magnetometer (VSM) revealed high saturation magnetization (M_s = 45.65 emu/g). The superparamagnetic property of MP-OHP was confirmed from the blocking temperature (T_B) determined from field cooled and zero field cooled magnetization, measured by superconducting quantum unit interference device (SQUID) magnetometry. The stability of the aqueous dispersion of MP-OHP nanocarriers was confirmed from its high zeta potential (−30.5 mV). The drug encapsulation efficiency (55.2 ± 4.8% w/w) and the drug loading content (0.10 ± 0.04 wt%) in MP-OHP nanocarriers were determined from corresponding platinum contents in OHP and MP-OHP batches measured by inductively coupled plasma mass spectrometry (ICPMS). These nanocarriers exhibited a sustained release of OHP in phosphate buffer solution maintained at pH 5.5 and 7.4, where the drug release profile satisfied a combination of diffusion and swelling controlled mechanism. The cytotoxicity effect of MP-OHP nanocarriers was studied on MIA-PaCa-2 (pancreas) cancer cell line, where the GI_{50} values were more than 5 mg/mL and it exhibited 10 folds higher cytoxicity than the equivalent concentration of free drug.

1. Introduction

Conventional chemotherapy has limitations due to non-selective binding of cytotoxic drug leading to biodistribution of the drugs to various organs in the body. Further, poor pharmacokinetic properties of these drugs demand repeated drug dosing at its maximum tolerated dose (MTD) to maintain a desirable drug concentration in the serum to achieve optimum therapeutic effect [16]. But concentrations of these cytotoxic drugs in the serum could exceed the tolerance level and due to its lack of non-specific distribution in human body, these drugs might exhibit severe toxicity to healthy cells and tissues as well [47]. This has prompted to innovative therapeutic strategies where the drug is delivered at a targeted pathological site [1,5]. Such targeted drug delivery would promote accumulation of active drug molecules at pathological areas [24]. In this regard, the concept of magnetic targeting by using superparamagnetic iron oxide nanoparticles (SPIONs) encapsulated in biodegradable polymers has been receiving tremendous interest [31]. It was noted that the clinical phase-1 trials on SPIONs loaded polymeric nanomaterials were non-toxic [29]. Ideally the magnetic carrier should be like a core-shell structure where SPIONs and drug constitute the core while the biodegradable polymer acts as a shell [48]. Significant studies on model drug loaded in magnetically functionalized polymeric nanoparticulates are reported [3,4,823]. In this regard, use of biocompatible and biodegradable natural polymers e.g. chitosan, has shown the potential to improve the therapeutic index [6]. In addition, reduction of the sizes of these polymeric magnetic carriers to a few 100 nm is desirable to promote enhanced permeation and retention (EPR) effect [30] and moreover such small carriers could be efficiently transported through biological pathways to remote pathological locations by capillary action using external magnetic field. The choice of polysaccharides is usually based on its efficiencies to load sufficient amount of drug and SPIONs, minimum leakage of drug and SPIONs during transportation, controlled or predictable drug release at the target site and biodegradability with either elimination or minimized toxicity of degraded products [2].

There has been considerable development of nanoparticulates of polysaccharide or protein loaded with model cytotoxic drugs like 5-fluorouracil, doxorubicin or platinum based compounds [14,21,34,37]. Due to better anti-tumor activities, polysaccharide nanocarriers loaded with platinum based drugs, e.g., cis-platin, oxaliplatin were explored [22,25]. These nanocarriers though

* Corresponding author. Tel.: +91 1332 285280; fax: +91 1332 286202.
E-mail addresses: duttafcy@iitr.ernet.in, rdotkdot@gmail.com (R.K. Dutta).

2211-2863/$ - see front matter © 2012 Elsevier B.V. All rights reserved.
http://dx.doi.org/10.1016/j.rinphs.2012.05.001

showed controlled drug release property, but did not comprise any targeting ability.

The purpose of this present work was to develop a model oral nanoscale anticancer drug delivery system targeted to pancreas. The delivery system is a magnetically functionalized pectin cross linked with Ca^{2+} nanostructures containing oxalate(trans-*l*-1,2-diaminocyclohexane) platinum(II), i.e., oxaliplatin, a third generation platinum based anti-cancer drug. The SPIONs (magnetite nanoparticles) are encapsulated in these pectin nanostructures to impart magnetic targeting ability as well as to confine the drug delivery system to localized areas for sustained drug delivery. We have chosen pectin as a biodegradable polymer as it is known to be an excellent matrix for oral administrated colon specific drug delivery [28,39,45], due to its resistance to protease and amylase [15] that are active in upper gastrointestinal (GI) tract. In-spite of excellent drug formulation properties of pectin, it has not been widely explored for developing nanocarriers based anti-cancer drug delivery system [46].

In the present study, oxaliplatin was chosen as the anti-cancer drug due to its better anti-tumor activities with lesser likelihood to develop drug resistance owing to cyclohexyldiamine group [17]. Furthermore, the oxalato-bidentate ligand contributes to hydrophilicity of the drug (water solubility of 6 mg/mL at 20 °C). Due to this it is more soluble in blood plasma and exhibits better efficacy than the less hydrophilic cis-platin or carboplatin. Moreover, clinical results of oxaliplatin are favorable for treating various types of cancers including the colorectal metastatic pancreatic cancer [20]. Usually, the efficacy of anticancer drug depends on the ability to target the drug at tumors, which is cumbersome for colon and pancreas. The targeting ability of our fabricated pectin nanocarriers loaded with OHP was induced by incorporating superparamagnetic iron oxide nanoparticles (SPIONs), preferably magnetite nanoparticles. The structural, morphological and magnetic properties of fabricated nanocarrier drug delivery system were characterized by various techniques. The in vitro drug release from these nanocarriers was studied at a different pH and its application as a targeted drug delivery was assayed against cancer cells.

2. Materials and methods

2.1. Materials

$Fe(NO_3)_3 \cdot 9H_2O$, $FeSO_4 \cdot 7H_2O$, liquid ammonia, anhydrous $Ca(OH)_2$ of Analytical Grade were procured from Merck, India and were used without further purification. Pectin with 65% to 70% degree of esterification was obtained from Hi-Media lab, India. Oxaliplatin (O9512-5MG) was procured from Sigma Aldrich (GmbH) Germany. The chemicals for preparing phosphate buffer solution at pH 5.5 and pH 7.4, comprised di-potassium hydrogen orthophosphate (K_2HSO_4), potassium dihydrogen orthophosphate (KH_2PO_4), sodium hydroxide and phosphoric acid (H_3PO_4), were procured from Merck, India. The acidic pH was maintained by adding dilute H_3PO_4. Dialysis membrane made up of regenerated cellulose with MWCO of about 3500 Da, was procured from Fisher Scientific Pittsburgh PA. Millipore water (resistivity of 18.1 MΩ cm at 25 °C) was used in all the experiments. All chemicals, reagents and experimental facilities needed for cell viability studies were provided by Tata Memorial Centre, Advanced Centre for Treatment Research and Education in Cancer (ACTREC) Mumbai (India).

2.2. Fabrication of pectin based magnetic nanocarrier drug delivery system.

5 mg of oxaliplatin (OHP) was mixed with 2.5 mL of Millipore water to prepare 2.0 mg/mL stock solution of OHP at pH 4. From this stock solution, 250 μL was mixed with 5 mL of 0.4% w/v pectin solution and was stirred for 1 h at room temperature. To this solution, 5 mL of a freshly prepared dispersion of magnetite nanoparticles (MNPs) synthesized by co-precipitation of 2:1 M ratio of $Fe(NO_3)_3 \cdot 9\,H_2O$ and $FeSO_4 \cdot 7\,H_2O$ with liquid ammonia [32] was added after conditioning the MNPs at pH 4. As chloride ions tend to form an inactive precipitate of 1,2-diaminocyclohexane platinum(II) complex [12], the pH of the reaction medium was maintained by dil. H_3PO_4. For the same reason, the pectin solution was cross-linked by adding 0.8% w/v solution of $Ca(OH)_2$ drop wise in acidic condition (pH ~ 4). In this study the composition of pectin and Ca^{2+} ions at pH 4 was kept 0.4% and 0.8% w/v, respectively, as optimized by us earlier [38]. The total volume of the reaction mixture (15.25 mL) comprising pectin, $Ca(OH)_2$ solution, freshly prepared MNPs and aqueous solution of oxaliplatin was stirred for 6 h at room temperature to allow the formation of calcium pectinate nanocarriers with MNPs and OHP encapsulated. This batch of sample will be referred here as MP-OHP nanocarriers, which were magnetically separated from the nanostructures of calcium pectinate without MNP encapsulation. The MP-OHP nanocarriers were purified by washing several times in phosphate buffer solution for removing loosely adhered drug and MNPs on the surface of the nanostructures. It may be remarked that negligible amount of MNPs might remain on the surface of calcium pectinate nanostructures as demonstrated by us earlier by X-ray photoelectron spectroscopy [38]. The MP-OHP nanocarriers were lyophilized for further studies. Similarly, a batch of calcium pectinate nanostructures were synthesized where MNPs were encapsulated along with oxaliplatin, and this batch of sample will be referred to as MP.

2.3. Methodology for drug loading analysis

The as-fabricated MP-OHP dispersion comprised of free dissolved drug (y) and drug loaded in MP-OHP nanocarriers (x). If the initial amount of the drug taken is w, then the drug loaded in MP-OHP nanocarriers is calculated as $x = w - y$. The concentration of free dissolved drug in the dispersion was determined by the bulk equilibrium reverse dialysis method [27]. The concentration of the drug was measured by inductively coupled plasma mass spectrometry (ICPMS). The drug loading content, i.e., the amount of loaded drug per weight of the MP-OHP nanocarrier (in wt%) was calculated as $(x/t) \times 100$, where t = weight of the fabricated MP-OHP. The % encapsulation efficiency of the drug in the nanocarrier is given as $(x/w) \times 100$.

2.4. Characterization

The X-ray diffraction (XRD) measurements of the fabricated MP-OHP and MNPs were performed with a powder diffractometer (Bruker AXS D8 Advance) using graphite monochromatized CuK_α radiation source. The morphology of the fabricated MP-OHP batch was studied by the transmission electron microscopy (TEM) operated at 200 kV FEI Technai-G^2 microscope and by the field emission scanning electron microscopy (beam resolution of 2 nm) with energy dispersive x-ray analyzer (FESEM-EDAX, FEI-Quanta 200 F) operated at 20 kV. The sample for TEM studies was prepared by dropping a diluted dispersion of MP-OHP nanocarriers on a carbon coated 150 mesh copper grid and dried at room temperature. Similarly for SEM studies, the diluted dispersion of MP-OHP was sprayed on a clean glass plate, dried in air and then coated with ultra-thin layer of Au. Dynamic light scattering (DLS) experiments were performed by using the Malvern Zetasizer Nano ZS90 instrument with a 4 mW He–Ne laser (633 nm wavelength) and a detector at a fixed angle of 173°. The DLS based size measurements were carried out in triplicate at 25 °C by transferring about 1 mL of dust free sample solution into

four-clear-size disposable polystyrene cell (Malvern). The zeta potentials (ξ) of the MP-OHP, pectin, OHP, MNP and MP batches were measured in triplicate at 25 °C by injecting 0.75 mL of dust free sample solution into disposable folded capillary cells (Malvern). The magnetic properties of the batches of MP-OHP, MP and MNP were recorded by vibrating sample magnetometer (VSM, Princeton applied Research Model 155) and by superconducting quantum unit interference device (SQUID) magnetometer (MPMSXL, USA). The magnetization measurements using VSM were recorded from the hysteresis loop of *M*–*H* curve in the range ± 10 kOe at room temperature. For SQUID measurement, a known amount of lyophilized samples were packed in diamagnetic capsules and were inserted in a polyethylene straw as a sample holder. The field cooled (FC) and zero field cooled (ZFC) measurements were recorded using SQUID at an applied field of 50 Oe by scanning between 5 and 300 K.

2.5. In vitro drug release

The dialysis bag diffusion technique was used to study the in vitro release of OHP from MP-OHP nanocarriers [41]. Briefly, the batches of MP-OHP nanocarriers were transferred to a dialysis bag, referred to as a donor compartment, containing 5 mL of freshly prepared phosphate buffer solution at pH 5.5 (without enzyme). This bag with its contents was then transferred to 20 mL of the buffer solution at pH 5.5 without enzymes (referred as receptor compartment) and gently stirred at 100 rpm for 40 h at 37.0 ± 0.1 °C in an incubator shaker. The choice of pH of 5.5 for the release study was to simulate mild acidic condition in the vicinity of tumor tissues [18]. In addition the pH of 5.5–5.7 also simulates that of the proximal colon for mimicking release of OHP from the fabricated nanocarriers at colon specific target [28]. In a similar manner the release of OHP from MP-OHP nanocarriers was performed in phosphate buffer solution at pH 7.4, without enzyme for 48 h to mimic the drug release in blood. About 1.5 mL of an aliquot was withdrawn from the respective receptor compartments at each specified time periods and was replaced with equal volume of fresh medium to mimic the sink conditions of the human body. The aliquot was centrifuged at 15000 rpm for 15 min and the supernatant liquid consisting of released drug was analyzed.

2.6. Methodology for drug analysis

The drug analysis was performed by measuring corresponding Pt concentration in the drug. Inductively coupled plasma mass spectrometry (ICPMS, Perkin Elmer Sciex, Elan DRC-e) was used for measuring Pt concentration, which was of the order of $\mu g\ mL^{-1}$ in the released media. This method is based on ionization of analyte by plasma and subsequent determination of ionic species in terms of mass/charge ratio using the mass spectrometry technique. First the analysis of Pt concentration was calibrated by measuring known standard platinum solutions (Merck, India) of concentrations of 50, 100, 250, 500 and 750 $ng\ mL^{-1}$, which corresponded to a linear fit of $R^2 = 0.988$ (Fig. S1a, given as supporting material). Next, calibration curve for estimating drug concentration in phosphate buffer solutions at pH 5.5 and 7.4 were plotted by measuring Pt concentration by ICPMS against known drug concentrations, e.g. 200 $ng\ mL^{-1}$, 350 $ng\ mL^{-1}$, 500 $ng\ mL^{-1}$, 750 $ng\ mL^{-1}$ and 1000 $ng\ mL^{-1}$. A linear fit with $R^2 = 0.993$ at pH 7.4 (Fig. S1b, given as supporting material) was obtained. Similarly, a linear correlation with $R^2 = 0.998$ at pH 5.5 was obtained, which indicated the validity of the method for measuring drug concentration by ICPMS. All the experiments were performed in triplicate and results are given as mean ± SD (SD = standard deviation).

2.7. Modeling of drug release

The mechanism of drug release from MP-OHP nanocarriers was studied using Korsemeyer–Peppas equation, given as $(M_t/M_\infty) = kt^n$, which can be expressed as $M_t/M_\infty \times 100 = (k \times 100) \times (t^n)$ [26], where $(M_t/M_\infty) \times 100$ corresponds to experimentally measured % cumulative drug release; M_∞ corresponds to 100% drug release, M_t corresponds to drug release at time (t), 'k' is a constant incorporating structural and geometric characteristics of material and 'n' is the diffusion exponent characteristic of release mechanism. For spheres, the value of $n < 0.43$ corresponds to drug release from the polymer matrix by Fickian diffusion [40]. Similarly, the value of 'n' in the range of 0.43–0.85 indicates diffusion controlled and swelling controlled drug release. While, $n > 0.85$ indicate swelling controlled drug release, attributed to polymer relaxation during swelling [44].

2.8. In vitro cell viability

The in vitro cytoxicity study of the batches of MP-OHP nanocarriers was assayed in MIA-PaCa-2 (pancreas) cancer cell line by sulforhodamine B (SRB) dye colorimetric assay [42,43]. The cell line was grown in RPMI 1640 medium containing 10% fetal bovine serum and 2 mM L-glutamine. In the screening experiment, 5000 cells were inoculated into 96 well microtiter plates in 100 μL media and incubated at 37 °C, 5% CO_2, 95% air and 100% relative humidity for 24 h. Ten microliters of MP-OHP nanocarriers of concentrations in the range of 1–5 mg/mL was suspended in phosphate buffer solution at pH 7.4 and incubated for 48 h. The assay was terminated by addition of cold trichloroacetic acid (TCA). The cells were fixed in situ by the gentle addition of 50 μL of cold 30% (w/v) TCA and incubated for 60 min at 4 °C. After discarding the supernatant, the plates were washed repeatedly with tap water and air dried. To each of the wells, a 50 μL sulforhodamine B solution (SRB), at 0.4% (w/v) in 1% acetic acid was added, and plates were incubated for 20 min at room temperature. After staining, the unbound dye was recovered and the residual dye was removed by washing repeatedly with 1% (w/v) acetic acid. The plates were air dried and the bound stain was subsequently eluted with 10 mM trizma base, and the absorbance was read on a microplate reader at a wavelength of 540 nm. Percent growth was calculated on a plate-by-plate basis for test wells relative to control wells, which is expressed as the ratio of average absorbance of the test well to the average absorbance of the control wells times 100. These experiments were performed in triplicate and the cell viability is given as mean ± standard deviation from triplicate analysis. Similarly, 10 μL solution of free OHP of concentrations e.g., 10, 20, 30, 40 and 50 μg/mL were treated to the respective cell cultures to assess the anti-proliferative effect of free drug to the cancer cells. As a control, 100 μL of PBS at pH 7.4 was added to the cells in eight of the wells. Growth inhibition of 50% (GI_{50}) was calculated from the drug concentration resulting into 50% reduction in the net protein increase, which was a measure of SRB staining during the incubation of cancer cells with drug. The cytotoxicity studies were performed in the authorized cancer research institute at Tata Memorial Centre, Advanced Centre for Treatment Research and Education in Cancer (ACTREC) Mumbai (India).

3. Results and discussion

3.1. Fabrication of MP-OHP nanocarriers

The fabrication of spherical nanocarriers of MP-OHP was confirmed from an array of characterization techniques. The

scanning electron microscopy (SEM) study revealed formation of spherical shaped MP-OHP nanocarriers with a size distribution ranging between 100 and 200 nm, in dry condition (Fig. 1, inset). The MNPs encapsulated in calcium pectinate nanostructures was evident from the observation of X-ray peaks characteristic to the compositional elements of MNPs (Fe K_α peak at 6.39 keV and Fe K_β peak at 7.10 keV) and that of calcium pectinate (Ca K_α peak at 3.63 keV) in the energy dispersive x-ray analysis (EDAX) spectrum of a representative nanostructure (Fig. 1). The X-ray peaks of Pt, corresponding to oxaliplatin, was not detected by EDAX as Pt content in the MP-OHP nanostructures was below the detection limits of Pt by EDAX (detection limit was about 500 $\mu g\, g^{-1}$). Further, the morphology of the as-fabricated MP-OHP nanostructures studied by transmission electron microscopy (TEM) confirmed the formation of 100–150 nm sized nanostructures (Fig. 2). The corresponding selected area electron diffraction (SAED) image showed concentric rings, which were due to the presence of polycrystalline SPIONs encapsulated in MP-OHP nanocarriers. The SPIONs encapsulated in MP-OHP were magnetite nanoparticles (MNPs), which is revealed from the peaks of the XRD pattern corresponding to 220, 311, 400, 511 and 440 planes (Fig. 3). Similar peaks were also detected in the XRD pattern recorded in the synthesized MNPs. These peaks are characteristic of the cubic magnetite structure as corroborated with the reported data in JCPDS (Joint committee on powder diffraction standards) card number 01-11111 and agreed well with our previous study of synthesis of MNPs encapsulated in calcium pectinate nanostructures [38]. The cross-linking of the carboxylic

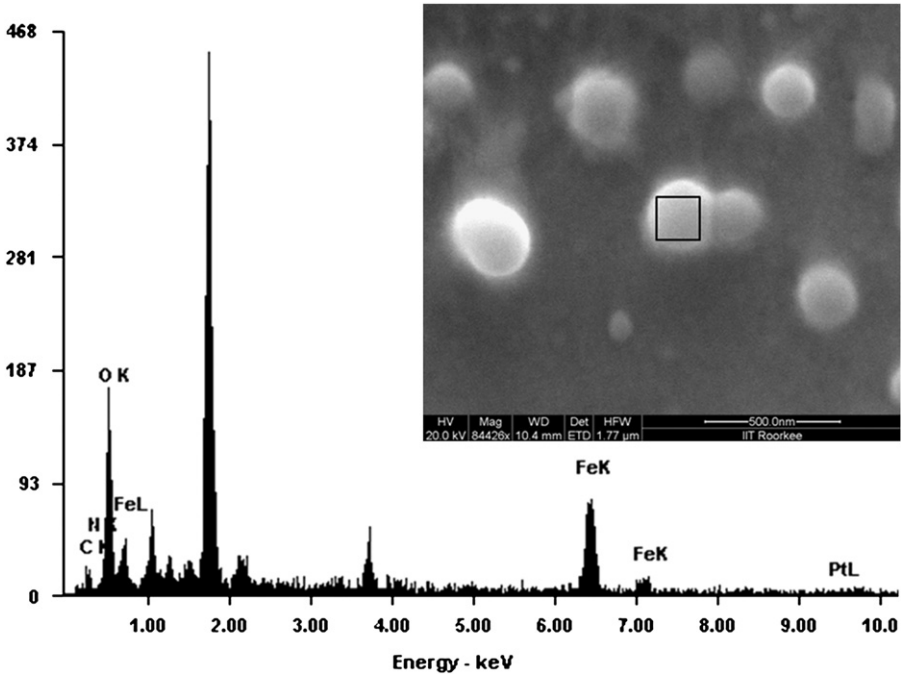

Fig. 1. Scanning electron microscopy of the MP-OHP nanocarriers showing spherical morphology of about 100–200 nm size (inset) and the energy dispersive X-ray analysis (EDAX) of a representative nanocarrier marked in the inset revealed co-localization of the characteristic K-x-rays of Fe and Ca as a marker of MNP encapsulated in calcium pectinate.

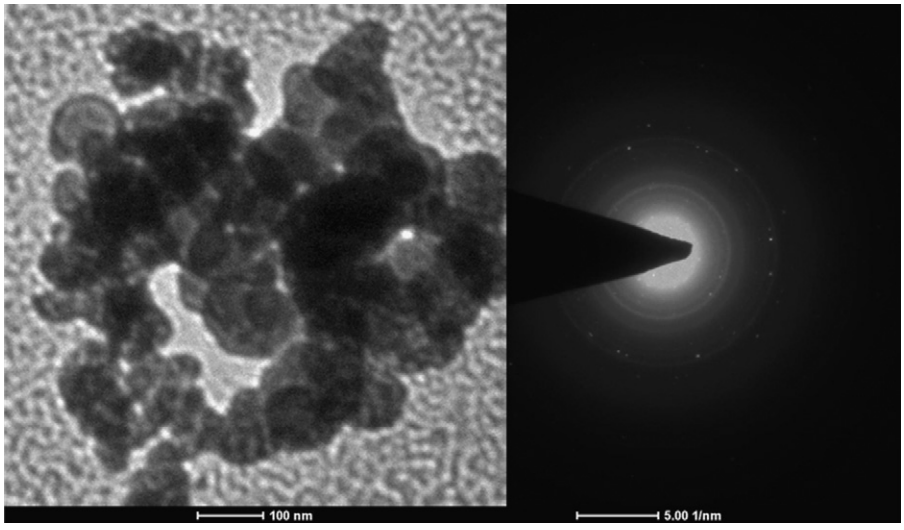

Fig. 2. Transmission electron microscopy (TEM) image showing 100 nm spherical MP-OHP nanospheres. The concentric circles observed in the SAED images adjacent to the TEM images correspond to encapsulated polycrystalline magnetite nanoparticles.

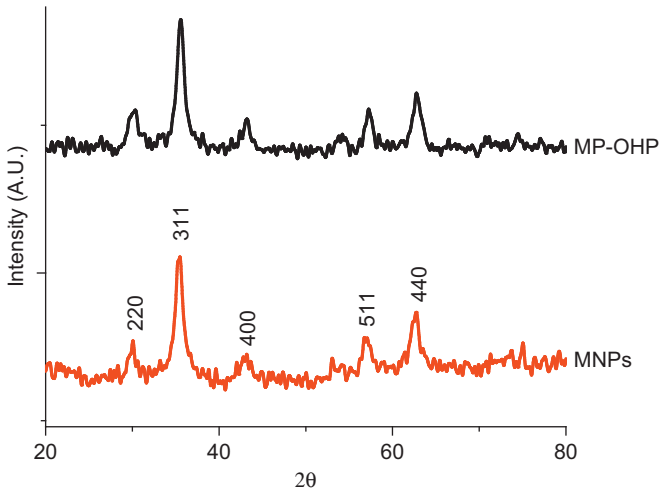

Fig. 3. X-ray diffraction pattern of MP-OHP showing all the peaks corresponding to magnetite nanoparticles (MNP), indicating encapsulation of MNPs in MP-OHP nanocarriers.

acid group of pectin by Ca^{2+} ions at the working pH 4, was substantiated from the measured zeta potential (ξ) given as mean value $\pm$ standard error of mean from triplicate measurements. The ξ of pectin was measured as -36.1 ± 0.6 mV at pH 4, which indicated negative surface charge due to $-COO^-$ groups of pectin suitable for electrostatic interaction with Ca^{2+} ions, suggested for the egg-box model for preparation of calcium pectinate structures [13]. Further, the zeta potential of MNPs at pH=4 was $+17.6 \pm 0.4$ mV and its encapsulation in pectin nanostructure was likely to be electrostatic in nature. However, the ξ value of OHP at pH 4 was measured as -35.2 ± 0.5 mV and hence its encapsulation in pectin nanostructure could not be attributable to electrostatic phenomenon. It may be assumed that the negative surface charge of OHP interacted with the positive surface charge of MNPs at pH 4, which was then encapsulated in pectin network to form a stable MP-OHP nanostructure. The stability of the aqueous dispersion of the synthesized MP-OHP in aqueous medium was corroborated from its measured zeta potential of -30.5 ± 0.4 mV. The OHP encapsulation efficiency was measured as $55.2 \pm 4.8\%$ (w/w) of the initial amount of drug treated, and the loading content of OHP was 0.10 ± 0.04 wt% of the fabricated MP-OHP nanocarriers. From these investigations, it is evident that oxaliplatin and MNPs were successfully encapsulated in pectin based nanostructures.

3.2. Magnetic properties of MP-OHP

The magnetic property of the fabricated MP-OHP nanocarrier was studied by recording magnetization (M) values against applied magnetic field (H) at room temperature using VSM. The M–H curve of MP-OHP (Fig. 4a) exhibited negligible coercivity and remanence magnetization, and was similar to that of the as-synthesized MNPs and MP. This phenomenon was typically due to superparamagnetism, which is attributable to the magnetite nanoparticles [9] and is considered to be favorable for targeted drug delivery [36]. The saturation magnetization (M_s) of MP-OHP nanocarrier between ± 10 kOe was measured as 45.65 emu/g. The M_s value of MP-OHP was similar to that of the MP batch (without oxaliplatin encapsulation). However, the M_s values of MP-OHP and MP batches were 20% less than that of the as-synthesized MNPs (55.69 emu/g). The decrease in the M_s value in MP-OHP nanocarrier could be attributed due to the formation of magnetic dead layer by nonmagnetic materials, namely Ca^{2+} cross linked pectin at the domain boundary wall of MNPs [19]. The capability of maneuvering the dispersion of these MP-OHP nanocarriers by

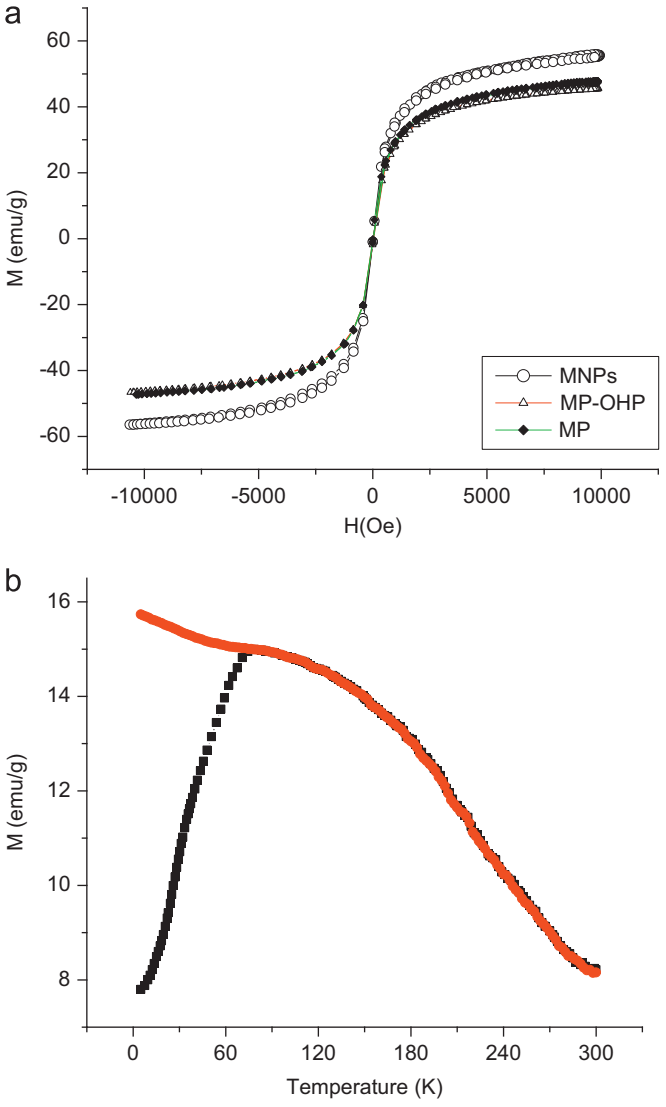

Fig. 4. (a) Magnetization vs. field (M–H) curve of MNPs, MP-OHP and MP batches measured by VSM at 10 kOe and at room temperature. (b) Superconducting quantum unit interference device (SQUID) measurement of MP-OHP batch nanocarriers recorded at 50 Oe showing divergence of magnetization curves corresponding to zero field cooled (ZFC, shown in black) and field cooled (FC, shown in red) plots, indicating superparamagnetism of the MP-OHP.

external magnet was observed (Fig. S2, given as supporting material). Further, the superparamagnetic behavior of MP-OHP nanocarrier was confirmed from the SQUID measurement by recording field cooled (FC) and zero field cooled (ZFC) magnetization at 50 Oe applied field in a temperature range between 5 and 300 K (Fig. 4b). The blocking temperature (T_B), which is a characteristic feature of superparamagnetic materials that depends on the particle size, was determined to be 78.2 K from the point of divergence of the FC and ZFC plots. Notably, the blocking temperature value corroborated well with the reported literature of superparamagnetic iron oxide nanoparticles [32].

3.3. In vitro drug release assay

A time dependent cumulative release of OHP from MP-OHP nanocarriers was observed in phosphate buffer at pH 5.5 (Fig. 5a) and at pH 7.4 (Fig. 5b). About 90% of the loaded OHP in MP-OHP was released in 24 h at pH 5.5. A detailed analysis of drug release however, revealed 23% release in 0–1 h, and 63% of loaded OHP was

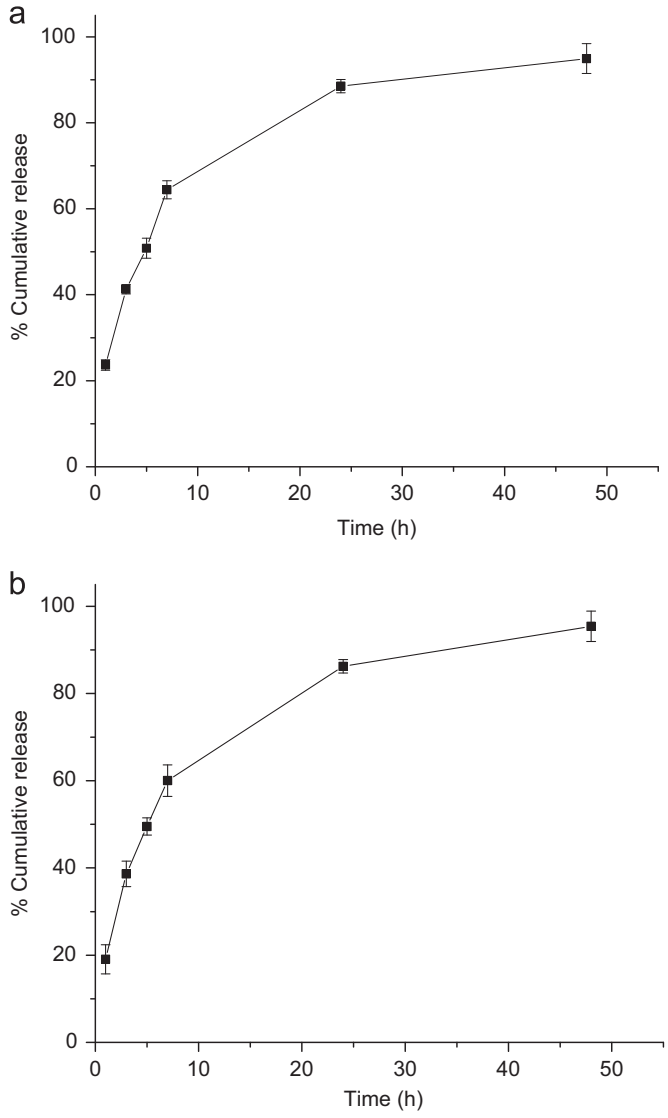

Fig. 5. (a) Showing in vitro release of OHP from MP-OHP nanocarriers up to 48 h in phosphate buffer solution kept at pH 5.5. (b) Showing in vitro release of OHP from MP-OHP nanocarriers up to 48 h in phosphate buffer solution kept at pH 7.4.

release in 0–7 h. Similarly, the time dependent release pattern of OHP at pH 7.4 was analogous to that observed for pH 5.5. About 84% of the loaded OHP was released in 24 h at pH 7.4 and about 95% was released in 48 h. Our results were similar to the release patterns of cis-platin from PLGA-PEG nanoparticles [11]. The detailed analysis of drug release pattern at pH 7.4 revealed ~19% release during the first hour and about 60% of cumulative release was recorded in 7 h. Notably the rate of drug release was substantially high at pH 5.5 and at 7.4. It necessitates rapid transport of the MP-OHP nanocarriers to targeted site to minimize drug leakage at unwanted sites. Due to the encapsulation of SPIONs, the MP-OHP nanocarriers could be transported by applying external magnetic field and achieve a time dependent sustained release at a targeted site.

3.4. Drug release mechanism

A plot of cumulative drug release (%) in logarithmic scale, given as $(\log M_t/M_\infty) \times 100$ against log t, for t = 7 h at pH 5.5 (Fig. 6a) and 7.4 (Fig. 6b), revealed linear fit with $R^2 = 0.9955$ and 0.9967 respectively. The factor '*n*' was determined from the slopes of the fit as 0.5018 and 0.5886 respectively, for release at pH 5.5 and 7.4.

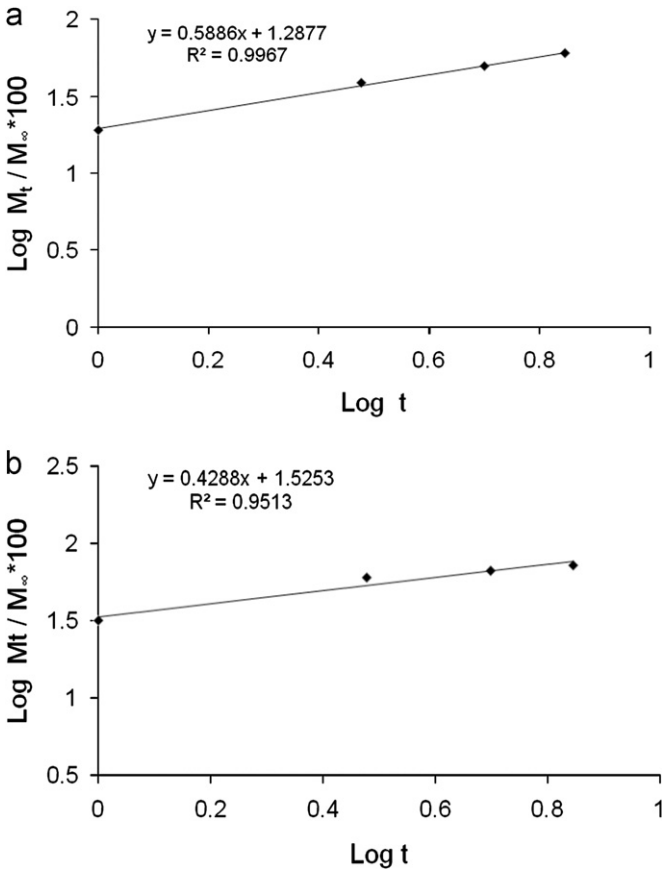

Fig. 6. (a) Showing linear fit of in vitro release of OHP up to 7 h from MP-OHP nanocarriers in phosphate buffer solution at pH 5.5, using Korsemayer–Peppas equation in log scale. (b) Showing linear fit of in vitro release of OHP up to 7 h from MP-OHP nanocarriers in phosphate buffer solution at pH 7.4, using Korsemayer–Peppas equation in log scale.

These values of '*n*' indicated non-Fickian transport, where the drug release could be considered to be due to combination of diffusion as well as swelling controlled and corroborated well with literature reports [40]. The parameter '*k*' was estimated from the intercepts of the plots as 0.236 and 0.194 respectively, from the drug release data in pH 5.5 and 7.4. Notably, the '*n*' and '*k*' values determined by us were in good agreement with polymeric microparticulate based drug delivery system [44]. The possible swelling effect of pectin nanocarrier in phosphate buffer solution at pH 5.5 and 7.4 was indicated in the dynamic light scattering (DLS) measurement. The average size of MP-OHP at pH 5.5 and at 7.4 were similar and was measured to be 330 ± 110 (Fig. 7), which was nearly two fold higher than their corresponding dried samples as measured by SEM and TEM. It is however not conclusive if the size distribution of MP-OHP nanocarriers measured by DLS is due to swelling effect or due to particle aggregation. It may be argued that MP-OHP most likely swelled in phosphate buffer solution and facilitated drug release, as supported by the swelling controlled release mechanism. Similar swelling controlled release from calcium pectinate beads loaded with drug was reported earlier [10]. The observed swelling can be due to repulsion of increased number of carboxylate groups in pectin ($pK_a = 2.9–4.1$) which are likely to weaken the calcium pectinate structure [33].

3.5. Cell viability assay of MP-OHP

The cytotoxicity study of the as fabricated MP-OHP nanocarriers dispersed in pH 7.4 was studied in MIA-PaCa-2 pancreas cancer cell lines by SRB assay. By treating increasing concentration of 1–5 mg/mL

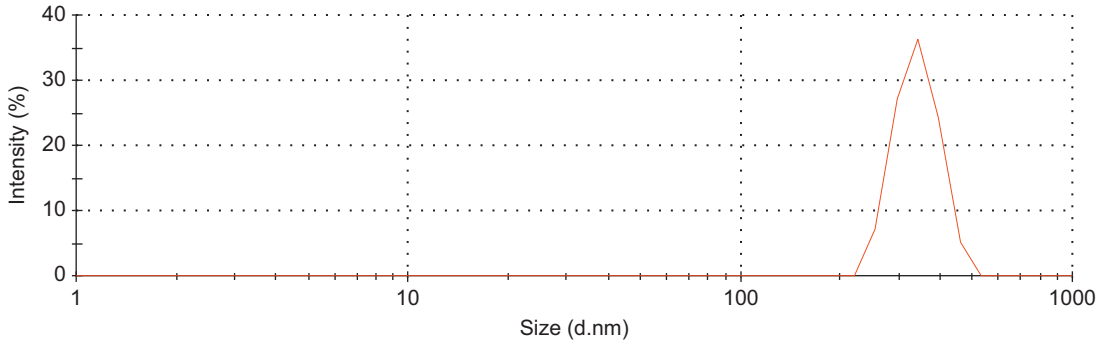

Fig. 7. Dynamic Light Scattering (DLS) measurement of MP-OHP nanocarriers in aqueous medium at pH 5.5 showing average particulate size of the order of 330 nm due to swelling effect.

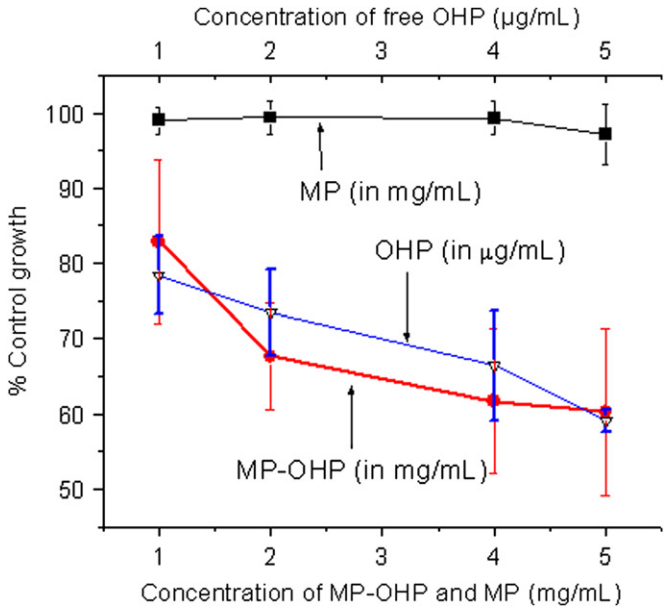

Fig. 8. In vitro cell viability study for MP-OHP nanocarrier, MP and free OHP in MIA-PaCa-2 (pancreas) cancer cell lines after 48 h interaction by SRB assay.

dispersion of MP-OHP nanocarriers, a systematic decrease in the cell viability (%) was observed in MIA-PaCa-2 cancer cells (Fig. 8) and the corresponding GI_{50} was estimated to be above 5 mg/mL. About 40% inhibition of cancer cell growth was observed for the batch treated with 5 mg/mL MP-OHP. The cytotoxic behavior of MP-OHP was compared with free OHP drug of concentration 10–50 µg/mL. The cell viability pattern for free OHP was similar to that of the MP-OHP treated batch (Fig. 8), and the GI_{50} of free OHP was estimated to be more than 50 µg/mL. Since the batch MP (without drug) did not exhibit cytotoxicity (Fig. 8), therefore the decrease in cell viability for MP-OHP nanocarriers in MIA-PaCa-2 cells was definitely due to cytotoxic properties of the released OHP drug in the culture medium at pH 7.4.

From drug loading analysis, it was derived that the drug loading content in MP-OHP nanocarriers was about 0.1 wt%. In the case of 95% drug release in 48 h, the corresponding concentration of the released drug would be 10 fold lower than the free drug, but the extent of cell viabilities for both were nearly similar. This indicated higher cytotoxicity of MP-OHP nanocarriers towards pancreas cancer cells. A similar kind of enhancement in cytotoxicity towards cancer cells has been discussed for doxorubicin loaded in nanoparticles [35]. Compared to free oxaliplatin, the higher ability of inhibiting the growth of pancreas cancer cells by MP-OHP could be attributed to higher availability or retention of MP-OHP nanocarriers with cancer cells. The higher drug availability could be related to the sustained nature of drug delivery, as observed at pH 7.4 and also at pH 5.5. However, further studies on the therapeutic efficacy of our developed MP-OHP nanocarriers should be carried out on animal models in order to realize its clinical relevance of magnetically targeted cancer therapy.

4. Conclusions

A novel oxaliplatin encapsulated in magnetically functionalized spherical pectin nanocarriers of 100–200 nm sizes (MP-OHP) has been successfully fabricated. The encapsulation of magnetite nanoparticles in MP-OHP imparted superparamagnetic property, favorable for targeted drug delivery applications. In aqueous medium, the average size of the nanocarriers was 330 nm, which was suitable for achieving enhanced permeation and retention (EPR) in tumors. A reasonably high encapsulation efficiency of oxaliplatin was achieved in these pectin based magnetic nanocarriers. The drug release from the nanocarriers was sustained at pH 5.5 and 7.4 and attributed to a mixed effect of diffusion and swelling controlled release mechanism, based on Korsemeyer–Peppas model. Though the GI_{50} of MP-OHP in pancreas cancer cell was above 5 mg/mL, it exhibited 10 folds higher cytotoxicity effect than the free oxaliplatin, which has been attributed to sustained release of OHP from MP-OHP nanocarriers. The potential application of MP-OHP nanocarriers as clinically relevant magnetic nanocarrier for targeted cancer therapy has to be confirmed from further studies on animals models.

Acknowledgments

One of the authors (S.S) likes to acknowledge Ministry of Human Resource Development (MHRD), Govt. of India and IIT Roorkee for awarding senior research fellowship to carry out this work. We also acknowledge the Institute Instrumentation Centre, IIT Roorkee and Centre of Nanotechnology, IIT Roorkee for utilization of several instrumental facilities used in this study.

Appendix A. Supporting information

Supplementary data associated with this article can be found in the online version at http://dx.doi.org/10.1016/j.rinphs.2012.05.001.

References

[1] Akbulut M, D'Addio SM, Gindy ME, Prud'homme RK. Novel methods of targeted drug delivery: the potential of multifunctional nanoparticles. Expert Review of Clinical Pharmacology 2009;2:265–282.

[2] Arias JL. Novel strategies to improve the anticancer action of 5-fluorouracil by using drug delivery system. Molecules (Basel, Switzerland) 2008;13: 2340–2369.
[3] Arias JL, López-Viota M, López-Viota J, Delgado AV. Development of iron/ ethylcellulose (core/ shell) nanoparticles loaded with diclofenac sodium for arthritis treatment. International Journal of Pharmaceutics 2009;382: 270–276.
[4] Butescu N, Jordan O, Burdet P, Stadelmann P, Petri-Fink A, Hofmann H, et al. Dexamethasone-containing biodegradable superparamagnetic microparticles for intra-articular administration: Physicochemical and magnetic properties, in vitro and in vivo drug release. European Journal of Pharmaceutics and Biopharmaceutics: Official Journal of Arbeitsgemeinschaft fur Pharmazeutische Verfahrenstechnik eV 2009;72:529–538.
[5] Chari RV. Targeted cancer therapy: conferring specificity to cytotoxic drug. Accounts of Chemical Research 2008;41:98–107.
[6] Coviello T, Matricardi P, Marianecci C, Alhaique F. Polysaccharide hydrogels for modified release formulations. Journal of Controlled Release: Official Journal of the Controlled Release Society 2007;119:5–24.
[8] Dames P, Gleich B, Flemmer A, Hajek K, Seidl N, Wiekhorst F, et al. Targeted delivery of magnetic aerosol droplets to the lung. Nature Nanotechnology 2007;2:495–499.
[9] Daou TJ, Pourroy G, Bégin CS, Grenèche JM, Ulhaq BC, Legaré P, et al. Hydrothermal synthesis of monodisperse magnetite nanoparticles. Chemistry of Materials: A Publication of the American Chemical Society 2006;18: 4399–4404.
[10] Das S, Ng KY. Resveratrol-loaded calcium-pectinate beads: effects of formulation parameters on release and bead characteristics. Journal of Pharmaceutical Sciences 2010;99:840–860.
[11] Dhar S, Gu FX, Langer R, Farokhz OC, Lippard. SJ. Targeted delivery of cisplatin to prostate cancer cells by aptamer functionalized Pt(IV) prodrug-PLGA–PEG nanoparticles. Proceedings of the National Academy of Sciences 2008;105: 17356–17361.
[12] Edgar, S, Bernd, M, Stefan, P. US Patent Application no. 20060063720. Oxaliplatin solution concentrate. Filed on September 22 2004. Published on; March 23 2006.
[13] El Gibaly I. Oral delayed release system based on Zn-pectinate gel (ZPG) microparticles as an alternative carrier to calcium pectinate beads for colonic drug delivery. International Journal of Pharmaceutics 2002;232:199–211.
[14] Elzoghby AO, Samy WM, Elgindy NA. Albumin-based nanoparticles as potential controlled release drug delivery systems. Journal of Controlled Release: Official Journal of the Controlled Release Society 2012;157:168–182.
[15] Englyst HN, Hay S, MacFarlane GT. Polysaccharide breakdown by mixed populations of human faecal bacteria. FEMS Microbiology Ecology 1987;95: 163–171.
[16] Frei E, Elias A, Wheeler C, Richardson P, Hryniuk W. The relationship between high-dose treatment and combination chemotherapy: the concept of summation dose intensity. Clinical Cancer Research: An Official Journal of the American Association for Cancer Research 1998;4:2027–2037.
[17] Di Francesco AM, Ruggiero A, Riccardi R. Cellular and molecular aspects of drugs of the future: oxaliplatin. Cellular and Molecular Life Sciences: CMLS 2002;59:1914–1927.
[18] Fukamachi T, Chiba Y, Wang X, Saito H, Tagawa M, Kobayashi H. Tumor specific low pH environments enhance the cytotoxicity of lovastatin and cantharidin. Cancer Letters 2010;297:182–189.
[19] Gupta AK, Gupta M. Synthesis and surface engineering of iron oxide nanoparticles for biomedical applications. Biomaterials 2005;26:3995–4021.
[20] Ibrahim A, Hirschfeld S, Cohen MH, Griebel DJ, Williams GA, Pazdur R. FDA drug approval summaries: oxaliplatin. The Oncologist 2009;9:8–12.
[21] Jain A, Jain SK. In vitro and cell uptake studies for targeting of ligand anchored nanoparticles for colon tumors. European Journal of Pharmaceutical Sciences: Official Journal of the European Federation for Pharmaceutical Sciences 2008;35:404–416.
[22] Jain A, Jain SK, Ganesh N, Barve J, Beg AM. Design and development of ligand-appended polysaccharidic nanoparticles for the delivery of oxaliplatin in colorectal cancer. Nanomedicine: Nanotechnology, Biology and Medicine 2010;6:179–190.
[23] Kayal S, Ramanujan RV. Doxorubicin loaded PVA coated iron oxide nanoparticles for targeted drug delivery. Materials Science Engineering 2010;30: 484–490.
[24] Kim S, Kim JY, Huh KM, Acharya G, Park K. Hydrotropic polymer micelles containing acrylic acid moieties for oral delivery of paclitaxel. Journal of Controlled Release: Official Journal of the Controlled Release Society 2008;132:222–229.
[25] Kim J-H, Kim Y-S, Park K, Lee S, Nam HY, Min KH, et al. Antitumor efficacy of cisplatin-loaded glycol chitosan nanoparticles in tumor-bearing mice. Journal of Controlled Release: Official Journal of the Controlled Release Society 2008;127:41–49.
[26] Korsmayer RW, Gurny R, Doelker E, Buri P, Peppas NA. Mechanisms of solute release from porous hydrophilic polymers. International Journal of Pharmaceutics 1983;1983(15):25–35.
[27] Levy MY, Benita S. Drug release from submicronized o/w emulsion: a new in vitro kinetic evaluation model. International Journal of Pharmaceutics 1990;66:29–37.
[28] Liu L, Fishman ML, Kost J, Hicks KB. Pectin-based systems for colon specific drug delivery via oral route. Biomaterials 2003;24:3333–3343.
[29] Lübbe AS, Bergemann C, Huhnt W, Fricke T, Riess H, Brock JW, et al. Preclinical experiences with magnetic drug targeting: tolerance and efficacy. Cancer Research 1996;56:4694–4701.
[30] Maeda H, Wu J, Sawa T, Matsumura Y, Hori K. Tumor vascular permeability and the EPR effect in macromolecular therapeutics: a Review. Journal of Controlled Release: Official Journal of the Controlled Release Society 2000;65:271–284.
[31] Mahmoudi M, Sant S, Wang B, Laurent S, Sen T. Superparamagnetic iron oxide nanoparticles (SPIONs): development, surface modification and applications in chemotherapy. Advanced Drug Delivery Reviews 2011;63:24–46.
[32] Mikhaylova M, Kim DK, Bobrysheva N, Osmolowsky M, Semenov V, Tsakalakos T, et al. Superparamagnetism of magnetite nanoparticles: dependence on surface modification. Langmuir: the ACS Journal of Surfaces and Colloids 2004;20:2472–2477.
[33] Ofori-Kwakye K, Fell JT. Biphasic drug release: the permeability of films containing pectin, chitosan and HPMC. International Journal of Pharmaceutics 2001;28:139–145 2001.
[34] Park JH, Saravanakumar G, Kim K, Kwon IC. Targeted delivery of low molecular drugs using chitosan and its derivatives. Advanced Drug Delivery Reviews 2010;62:28–41.
[35] Parveen S, Misra R, Sahoo SK. Nanoparticles: a boon to drug delivery, therapeutics, diagnostics and imaging. Nanomedicine: Nanotechnology, Biology and Medicine 2012;8:147–166.
[36] Peng X-H, Qian X, Mao H, Chen Wang AY, Nie Z, Shin D.M. S. Targeted magnetic iron oxide nanoparticles for tumor imaging and therapy. International Journal of Nanomedicine 2008;3:311–321.
[37] Qi J, Yao P, He F, Yu C, Huang C. Nanoparticles with dextran/chitosan shell and BSA/chitosan core—doxorubicin loading and delivery. International Journal of Pharmaceutics 2010;393:176–184.
[38] Sahu S, Dutta RK. Novel hybrid nanostructured materials of magnetite nanoparticles and pectin. Journal of Magnetism and Magnetic Materials 2011;323:980–987.
[39] Sande SA, Sungthongjeen S, Pitaksuteepong T, Somsiri A, Sriamornsak P. Studies on pectins as potential hydrogel matrices for controlled- release drug delivery. Drug Development and Industrial Pharmacy 1999;25:1271–1276.
[40] Siepmann J, Peppas NA. Mathematical modelling of controlled drug delivery. Advanced Drug Delivery Reviews 2001;48:139–157.
[41] Singh S, Muthu MS. Preparation and characterization of nanoparticles containing a typical antipsychotic agent. Nanomedicine: Nanotechnology, Biology, and Medicine 2007;2:233–240.
[42] Skehn P, Storeng R, Scudiero A, Monks J, McMohan D, Vistica D, et al. New colorimetric cytotoxicity assay for anticancer drug screening. Journal of the National Cancer Institute 1990;82:1107.
[43] Vichai V, Kirtikara K. Sulforhodamine B. Colorimetric assay for cytotoxicity screening. Nature Protocols 2006;1:1112–1116.
[44] Wang Q, Zhang J, Wang A. Preparation and characterization of a novel pH-sensitive chitosan-g-poly (acrylic acid)/ attapulgite/ sodium alginate composite hydrogel bead for controlled release of diclofenac sodium. Carbohydrate Polymers 2009;78:731–737.
[45] Wong TW, Colombo G, Sonvico F. Pectin matrix as oral drug delivery vehicle for colon cancer treatment. AAPS PharmSciTech 2011;12:201–214.
[46] Yu CY, Cao H, Zhang XC, Zhou FZ, Cheng SX, Zhang XZ, et al. Hybrid nanospheres and vesicles based on pectin as drug carriers. Langmuir: the ACS Journal of Surfaces and Colloids 2009;25:11720–11726.
[47] Yuan F, Qin X, Zhou D, Xiang Q-Y, Wang M-T, Zhang Z-R, et al. In vitro cytotoxicity, in vivo biodistribution and antitumor activity of HPMA copolymer–5-fluorouracil conjugates. European Journal of Pharmaceutics and Biopharmaceutics: Official Journal of Arbeitsgemeinschaft fur Pharmazeutische Verfahrenstechnik eV 2008;70:770–776.
[48] Zhang JL, Srivastava RS, Misra RDK. Core-shell magnetite nanoparticles surface encapsulated with smart stimuli-responsive polymer: synthesis, characterization, and LCST of viable drug-targeting delivery system. Langmuir: the ACS Journal of Surfaces and Colloids 2007;23:6343–6351.